

TRANSPARENT GENERATOR

Eric Carbonnier, PhD., Architect
University of Oregon/HMC Architects

G.Z. Brown, FAIA
University of Oregon

ABSTRACT

Windows reduce heat loss and heat gain by resisting conduction, convection, and radiation using thermal breaks, low-emissivity films, and window gaps. Contrary to advancing these resistive qualities, a highly conductive gap medium using Al_2O_3 nanoparticles dispersed in deionized water was used to enhance thermal conductivity. The solution harnessed the photothermal properties of Al_2O_3 nanofluids to trap, store, and transport thermally charged fluids to heat exchangers to preheat air and water, and to generate electricity forming a transparent generator—the Nanowindow. Seven Nanowindow prototypes with varying orders of air and fluid columns were fabricated and tested using distilled water (H_2O windows) to establish a baseline of performance, and then replaced with Al_2O_3 nanofluids. A solar simulator was built to avoid environmental radiant flux irregularities providing a uniform test condition averaging 750–850 W/m^2 . All Nanowindows were tested in a calibrated hot box determined to have a $\pm 4\%$ degree of accuracy based on four laboratory samples establishing a framework to conduct U-factor and solar heat gain coefficient (SHGC) measurements. Four heat exchange experiments and standardized window performance metrics (U-factor, SHGC, and visible transmission) were conducted on seven H_2O windows. The top performers were then tested using Al_2O_3 nanofluids. Nanowindows were coupled with thermoelectric generators generating a rated voltage of 0.31VDC/0.075ADC per $12in^2$ Nanowindow, an improvement of 38% over baseline. Standardized window performance metrics confirmed Nanowindow U-factors ranging from 0.23 to 0.54, SHGC from 0.43 to 0.67, and visible transmittance coefficient (VT) ranging from 0.27 to 0.38. The proof of concept experiment shifts window gaps from resisting energy to harnessing solar energy. The Nanowindow thus presents a unique opportunity to turn vast glass facades into transparent generators to offset energy demand, and reduce greenhouse gases.

INTRODUCTION

Windows aim to resist solar heat gain, infiltration, and limit energy transfer while maintaining high levels of visible transmittance, but rarely has a window achieved this balancing act and generated electricity. In Los Angeles, the last five high-rise buildings resulted in two million square feet of exterior glazing, and 1.3 million square feet with access to peak sun hours. With 1.3 million square feet of vertical real estate available for renewable generation not one development offered on-site renewable energy despite solar access and surface area availability.

The five developments resulted in a window-to-wall ratio of approximately 90%, and yet windows continue to be widely applied as a fenestration material of preference that offers aesthetic delight and transparency despite being directly attributed to energy consumption and carbon emissions (Aasteh & Selkiwitz, 1989). As window area increases so does the energy demand to heat and cool buildings. 22-32% of the building energy demand is attributed to poor window performance and results in 2 quads a year in energy or \$20 billion dollars. This results in an uptake in carbon emissions and greenhouse gases, and knowingly so, our affinity with glass continues to dominate the built environment.

Window performance is paramount in making a substantial impact on energy conservation measures, but some theorize that windows have reached their theoretical limit of performance (Johnson, 1991), yet the building industry continues to disregard these findings. Analyzing window performance through the lens of conduction, convection,

Eric Carbonnier, PhD., Architect, lectures at California Polytechnic University, Pomona, and Vice President of Sustainability at HMC Architects. **G.Z. Brown, FAIA**, Philip H. Knight Professor, Department of Architecture, Founding Director, Energy Studies in Buildings Laboratory

and radiation illustrates that modern windows resist these energy flows in the gap between panes, and it is within the gap that a divergent ideology emerges.

If windows have reached their theoretical performance limit, then what opportunities exist to expand a window’s capabilities? What if 1.3 million square feet of windows generated electricity without compromising solar heat gain, infiltration, and heat transfer while offering a high degree of visible transmittance? The physics of the window-sun relationship and the gap between panes was essential to answering these questions.

Background

The gap between panes was central to the experiment and resulted in a complex choreography of energy transfer considerations. To activate the gap’s electrical generation potential each energy domain was explored. It was theorized that the medium occupying the gap must retain high kinematic viscosity and low thermal conductivity (k) to maintain high insulating values (Johnson, 1991, p. 38). Heat transfer fluid were explored and naturally this increased convective traffic, and raised heat transfer across the glass panes. To offset this conductive transmission to the ambient, an air column was added to resist energy transfer between the fluid column and the ambient air. Conductivity (k) was largely dependent on the buoyancy flow of natural convection, the Rayleigh number¹, and higher conductivity values were beneficial to enhancing thermal exchange. Radiant energy was another opportunity to harness solar radiation. A low-e film was suspended in the gap to trap radiant energy rather than reflected to the ambient or to the surface of the glass (Figure 1). Collectively these strategies turned the gap in to an energy trap.

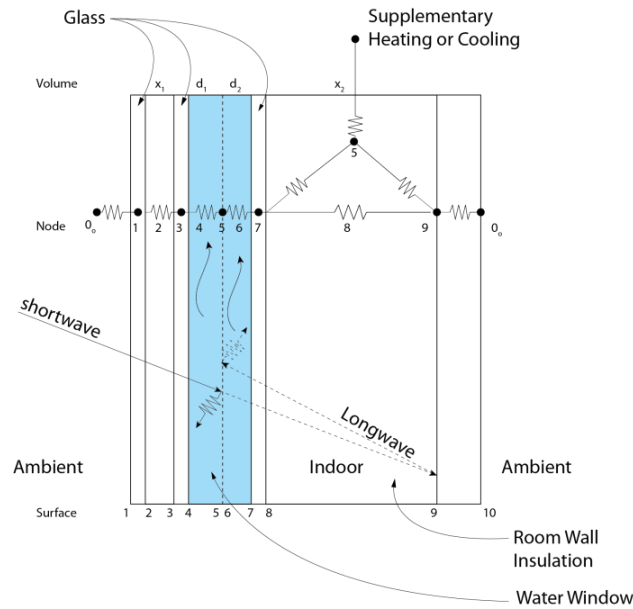


Figure 1 Energy Schematic

Nanofluids exhibited superior properties relative to those not only of conventional heat transfer fluids, but also of fluids containing micrometer-sized metallic particles (Choi, Zhang, Yu, Lockwood, & Grulke, 2001, p. 718). Thus the specific heat of water based fluids can be augmented by adding nanoparticles (Shin & Banerjee, 2011, p. 1), and that corresponding thermal conductivity can increase between 35%-45% (Shin & Banerjee, 2015, p. 898). Water based Al_2O_3 nanofluid’s specific heat decreases gradually as the nanoparticle volume fraction ϕ increases from 0.0% to 21.7% (Zhou & Ni, 2008, p. 92). The results indicated that the effective heat flow was influenced by volume

¹ Rayleigh number describes a fluids property when heat transfer occurs by conduction or convection.

fraction ϕ . Base fluids containing small amounts of nanoparticles resulted in increased thermal conductivity (Murshed, 2005, p. 372).

Öğüt (2009) investigated natural convection heat transfer of Cu, Ag, CuO, Al₂O₃, and TiO₂ water based nanofluids across a variable incline enclosure ranging from 0° to 90°. The test specimen was heated on one side with a constant heat flux, while the opposite was cooled, and all other sides adiabatic. Although the experiment focused on electronics and aerospace cooling solutions that require miniaturized solutions, the research draws parallels application to window environments. Similar to Timofeeva et. al., heat transfer rates increased with water based nanofluids, and as the solid volume fraction increases so does the conductive strength. This supports Timofeeva et. al. when mentioning that the 90nm particle was the highest thermally conducting performer. Additionally, the Rayleigh number (Ra) appears to exceed 1000 indicating that convection has started, and an excellent indicator that fluids will move by natural convection, and can be used to circulate nanofluids through heat exchangers. Öğüt concludes that aluminum and copper are the most effective heat transfer nanofluids.

Methods

Engineer a series of windows with fluid and air columns in varying configurations, and the ability to displace fluids to a heat exchanger and thermoelectric generator. Three factory tested windows (single pane, double pane, and triple pane) were acquired with accompanying window performance criteria. Seven Nanowindows with alternating fluid column, air gap, and suspended heat mirror in double pane, triple pane, and quad pane configurations were designed, fabricated, and tested for rate of heat loss (U-factor), visible transmittance (VT), and solar heat gain (SHGC), and electrical generation. A custom-built 0.5” window spacer fabricated from thermoplastic polycarbonate was engineered to accommodate sensors, fluid inlet/outlet, filling ports, expansion reservoir, and water tightness when fused with glass panes (Figure 2). The vision area of each window was 76% clear (Finlayson, Arasteh, Huizenga, Rubin, & Reilly, 1993, p. 3), and a fluid capacity of 0.94-liter (0.24-gallons). Two liters of Al₂O₃ nanofluids² with article size mean of 10 nm ± 5 nm in a concentration of 1% by weight in deionized water, and particle purity (metals basis) of 99.95+% was procured.

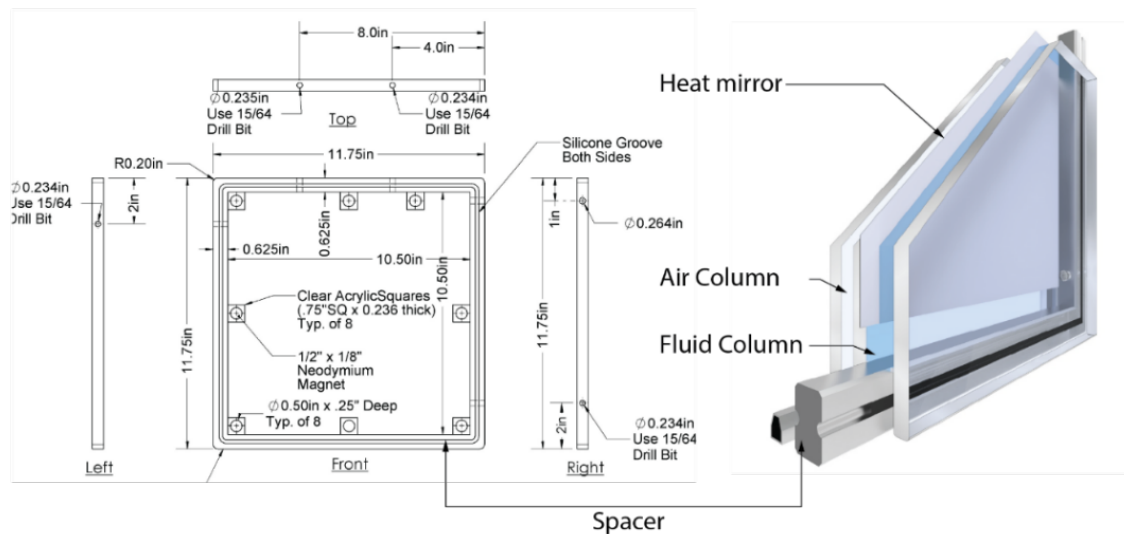


Figure 2 Window Spacer and Nanowindow #7 (only 1 of 7 illustrated)

² Nanofluids provided by Meliorum Technologies, Inc., 620 Park Ave. Ste. 145, Rochester, NY 14607 USA

A Solar Lab was built exclusively for testing the Nanowindow which offered uniform test conditions to limit variability between iterative experiments (Figure 3). The Solar Lab comprised of a low-cost solar simulator and a calibrated hot box (CHB) coupled with a data acquisition center using a Campbell Scientific equipment capable of sensor measurement, timekeeping, data reduction, programming, and actuation of fans, lights, heating & cooling system, and pumps.

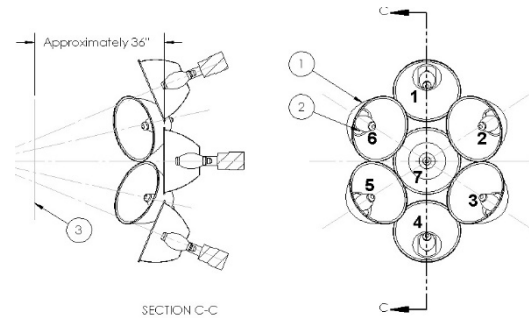
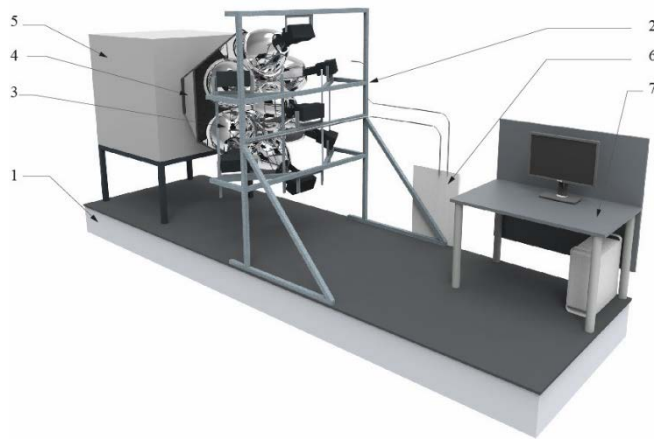


Figure 4 Array Geometry (1. Aluminum Spun Ellipsoidal Reflectors, 2. Metal Arc Lamps, 3. Test Plane)

Figure 3 Solar Lab (1. Lab Platform, 2 Array Rack, 3. Luminaires & Lamps 4. Concentrator, 5. Calibrated Hot Box, 6. Load Center, 7. Data Acquisition Center)

Using a parametric based solid modeler, the solar simulator was engineered to solve for maximum flux output based on various geometric positions to provide one sun at the test plane (Figure 4). Seven 400 watt MH400/U luminaires were selected and equipped with a SS VertX spun aluminum ellipsoidal 19-inch reflectors, and placed in a hexagonal concentrator fabricated from pre-mirror stainless steel to concentrate flux energy at the test surface.

A 4-foot cube (64ft³) Calibrated Hot Box (CHB) with a minimum sample area of 1ft² was fabricated according to ASTM's Standard Test Method for the Thermal Performance of Building Assemblies by Means of a Hot Box Apparatus (ASTM C1363-11). The CHB was composed of a climate chamber (proximal to the solar simulator), and meter chamber equipped with a heat source and a cooling system respectively.

EXPERIMENT

Three heat exchange experiments coupled nanofluids with air, water, and a thermoelectric generator (TEG³). Only the TEG experiment along with SHGC, U-Factor, and VT are reported here. Nanofluids were circulated from the Nanowindow to a 4 in² water block attached to a 3.88 in² TEG. The TEG was connected to a multimeter and measured electric potential (voltage) and Current (I) in direct voltage (DC) over the course of 4-hours. Tests compared water-based Nanowindows to Al₂O₃ Nanowindows.

Test 1 Thermoelectric Generator Only (H₂O only)

Test 2 Thermoelectric Generator + Heat Sink (H₂O only)

Test 3 Thermoelectric Generator Only (Al₂O₃ only)

Test 4 Thermoelectric Generator + Air Circulation, No Heat Sink (Al₂O₃ only)

³ Custom Thermoelectric Generator model 28711-5M31-12CW was procured. I_{max}(Amps)12.0, Q_{Max}(Watts)255.3, V_{max}(Volts)34.4

Test 5 Thermoelectric Generator + Heat Sink, No Air Circulation (Al₂O₃ only)

Test 6 Thermoelectric Generator + Heat Sink + Air Circulation (Al₂O₃ only)

Calibration

Solar simulator calibration was evaluated using Standard Specification for Solar Simulation for Photovoltaic Testing (ASTM E927-10) and International Electrotechnical Commission (IEC) standards. An Ocean Optics USB2000+VIS-NIR⁴ spectroradiometer compared the simulator's ultraviolet (UV), visible light (VIS), and near infrared (NIR) to ASTM G173 Terrestrial Reference Spectra. The calibration evaluated 100nm intervals from 350 to 1100nm wavelengths and resulted in a 2.3% temporal instability (ATSM Class B designation); Irradiance non-uniformity of <2% (ASTM Class B); and a spectral match 18% out of range of ASTM E927 criteria, but corrected using spectra specific filters to lower mismatch.

Heat transfer, flanking loss, and infiltration of the CHB was evaluated to characterize heat flow paths, and time to achieve steady state conditions. Three calibration exercises were performed and concluded that steady state was achieved in 2 hours with a 0.62°C differential swing in the climate chamber and a 0.79°C differential in the metering chamber which is less than the ±1°C allowed by ASTM and ISO standards. The hot box provided a climate chamber and metering chamber (Figure 5) capable of heating to 60°C and cooling to 10°C respectively. This condition offered the required differential between chambers of 22 °C (40 °F) which is the desired temperature differential for resistance testing (ISO 12567-1, 2010, p. 14).

To evaluate sample accuracy tested in the CHB three know samples (#0-polyiso, #1-single pane, #2-double pane, #3- triple pane glass) with laboratory certification for SHGC, VT, and U-Factor were tested. U-factor for the polyiso was 8% less compared to the certified value; single pane was 10% less; double pane was 4%, and triple pane was 3% more than the certified value. While the results averaged below 6%, a guarded hot box would have been desirable along with a slight suction in the climate chamber to prevent cold air from infiltrating into the meter chamber and impacting the overall energy balance (Burch, Licitra, & Zarr, 1990, p. 36).

The Solar Lab was equipped with sensors specific to understanding heat transfer, spectroscopy, and energy generation (Figure 5). An Apogee UV sensor SU100 was used to measure the light intensity from 250nm to 400nm; a hemispherical Hukseflux LP02 Solar Radiation Pyranometer⁵ was selected for its compatibility with measuring lamp based solar simulator in-situ experiments; Ocean Optics USB2000+VIS-NIR to measure ultraviolet, visible, and near infrared (UV-Vis-NIR) wavelengths from 350 to 1100 nm; and thermistor ambient temperature sensors, probe temperature sensors, and surface sensors.

⁴ USB2000+VIS-NIR is equipped with a silicon Sony ILX511B detector, 2048 pixels, pixel size of 14 μm x 200 μm, and pixel depth of ~62,500 electrons.

⁵ Hukseflux LP02 Pyranometer is a hemispherical solar radiation sensor with calibration uncertainty ±0.21x10⁻⁶ v/(W/m²).

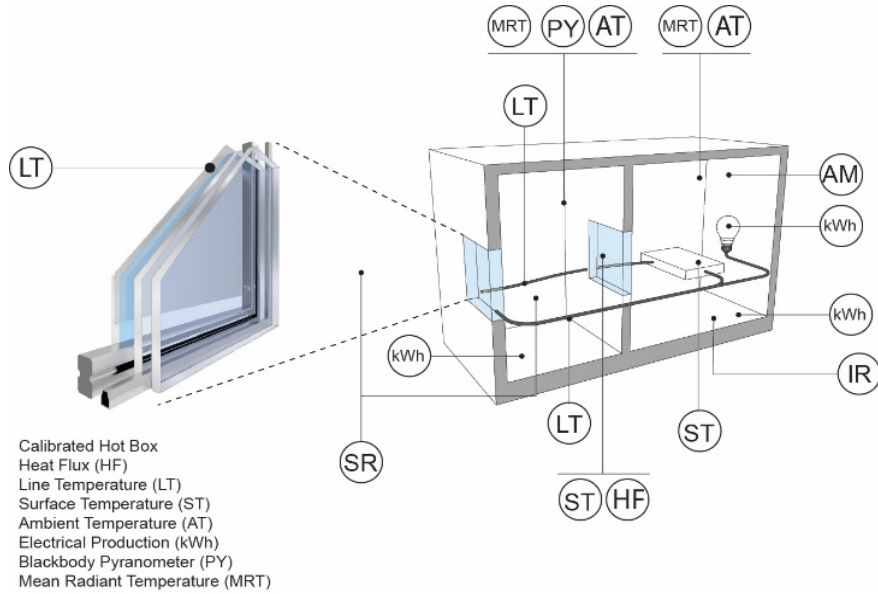


Figure 5 Calibrated Hot Box and Sensor Type and Placement

RESULTS

U-factor, VT, SHGC, and electrical generation of seven H₂O Nanowindow and Al₂O₃ Nanowindows were compared. Three factory built baseline windows (single pane, double pane, and triple pane) were also included in the analysis to compare known high performance windows to the Nanowindows.

U-factor for H₂O Nanowindows 7, 8, 9, and 10 offered promising results compared to factory double pane and triple pane windows (Figure 6) using Equation 1. The U-factor for Nanowindow 7 and H₂Owindow 7 were within ± 0.013 Btu/(hr) (ft²)(°F) of each other, and Nanowindow 8 and H₂Owindow 8 were ± 0.009 Btu/(hr) (ft²)(°F) of each other. Based on the CHB's accuracy it was deemed that Al₂O₃ Nanowindows had little to no impact on thermal resistance and nearly equal to H₂O Nanowindows.

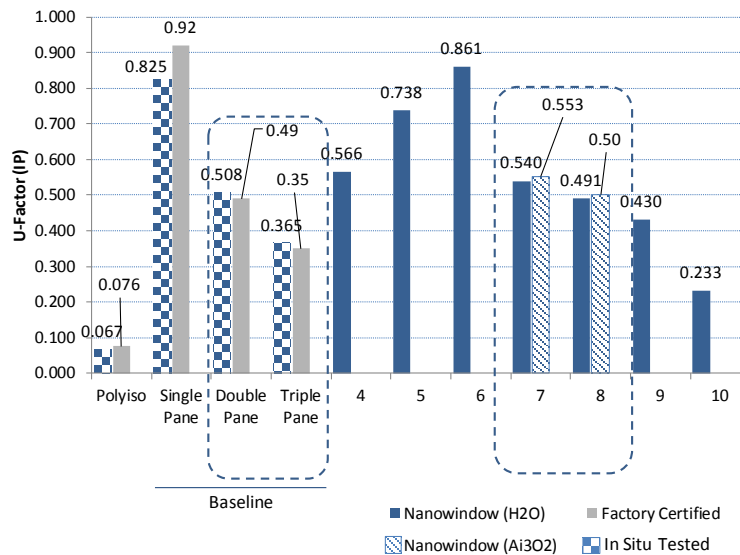


Figure 6 H₂Owindow U-factor Results

Visible Transmittance was calculated using ANSI/NFRC 200-2014 standards to establish a relative baseline of comparison, and it was determined that H₂O Nanowindow 7 and 8 were above the minimum criteria with a VT of 0.47 and 0.51 respectively, both of which are well above the 0.42(42%) VT code compliance for fixed windows. Nanowindow 7 and 8 resulted in 0.27 and 0.23 respectively which is below International Energy Conservation Code compliance (Figure 7).

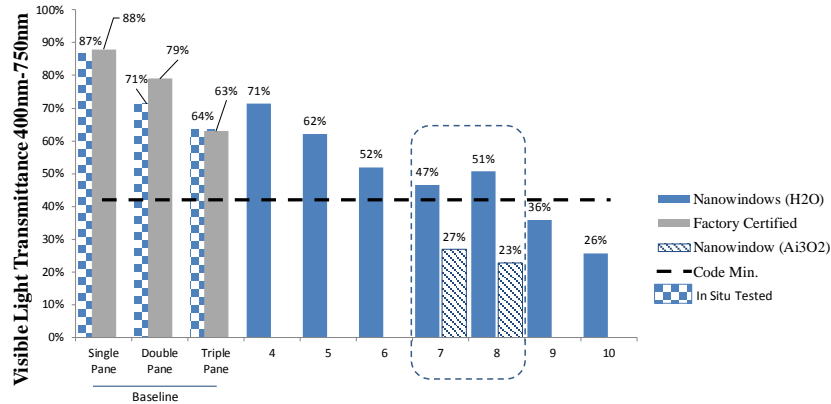


Figure 7 Nanowindow VT Results

H₂O Nanowindows 7,8, 9 and 10 Solar Heat Gain Coefficient (SHGC) yielded favorable results (Figure), but H₂O Nanowindows 7 and 8 resulted in comparable results to double pane and triple pane windows while H₂O Nanowindows 9 and 10 outperformed all the baseline windows. Nanowindow 7 was within ± 0.007 (1% difference) of baseline window 7, and the SHGC for Nanowindow 8 was surprisingly 0.049 or 7% more than baseline window 8 (Figure 8). This raised concerns that a testing error may had occurred as the rate of heat transfer between baseline window 8 and Nanowindow 8 should be similar. After closer examination of the data it was determined that the Climate Chamber had cooled beyond its set-point by 5°C reaching a low of 10°C compared to other test conditions that ran at a steady state of $\pm 15^\circ\text{C}$.

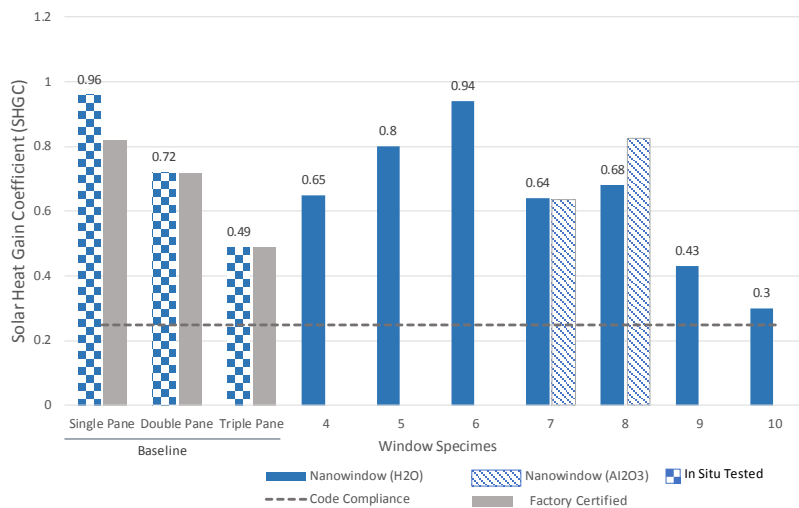


Figure 8 SHGC Results

Al₂O₃ Nanowindows 7 and 8 illustrated the most favorable results so the thermoelectric generator (TEG)

experiment focused on these two Nanowindows, and applied six tests. Test 1, the ambient temperature in climate chamber was unregulated for the first half of the experiment, and then cooled to 22°C to simulate a workplace environment. As expected, when the temperature differential across the thermoelectric generator (TEG) was increased so did the power and current output. Test 1 resulted on average ~0.022 vdc. System Size Factor (SSF) was used to determine system size relative to the desired voltage output to the actual voltage output to determine scaling efficiencies. The lower the SSF the more efficient the system regarding heat transfer and energy generation. This resulted in a SSF of 545 (12 vdc/.022 vdc) which was then applied to the TEG area and Nanowindow recognizing that transmission loss and individual system efficiencies were not taken into consideration at this stage.

Based on a 545 SSF to achieve a 12 vdc system would require 2,114 in² (14.6ft²) TEG coupled with 545ft² of water based Nanowindows. Test 2 increased the temperature delta between the TEG and the water block using an aluminum heat sink. The power output increased significantly to 0.036 volts and resulted in a system size factor of 333 which was 38% better than Test 1. Thus a 12 vdc system would need 1,292 in² of TEG coupled with 333ft² of nanowindow.

Tests 3-6 shifted to Al₂O₃ nanoparticles and resulted in increased voltage outputs as a function of larger temperature differential across the TEG as a function of the nanofluids. Test 3 resulted in 0.047volts - a 113% improvement over Test 1.

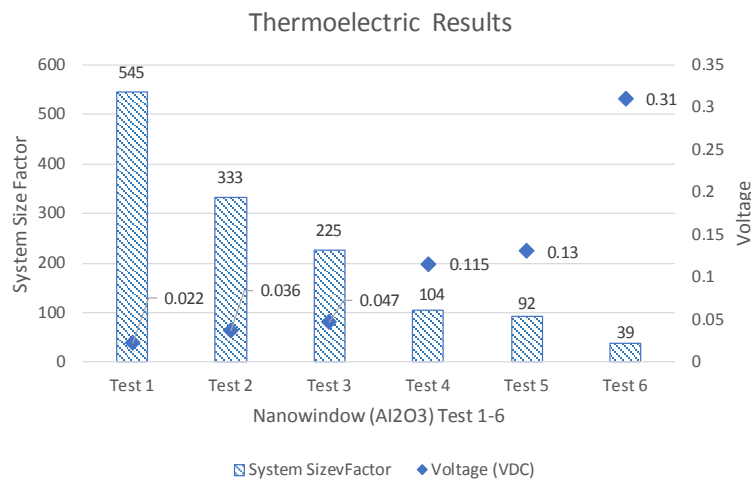


Figure 9 TEG Results

Test 6 generated 0.31volts and a rated current of 0.075Adc. This resulted in a System Size Factor (SSF) of 39 which was significantly better compared to all other water-based and nanoparticle Nanowindows (Figure 9, Test 6). Thus 151 in² (1.04ft²) of thermoelectric generator is required for every 39ft² of nanowindow system based on a system size factor of 39.

CONCLUSION

The gaps between seven prototype windows were filled with aluminum oxide (Al₂O₃) nanofluids. The nanofluids were circulated to a thermoelectric generator to determine the electrical production potential, and evaluated U-factor, VT, SHGC. U-factor performance diminished as a function of increase in conductivity, but on its own was an advantage that had to be balanced with power production. Visible transmission (VT) was less than favorable because of the nanoparticle weight to volume of concentration. Further nanotechnology investigation is required to determine appropriate concentration and sonication to agitate nanoparticle dispersion in the distilled water to improve optical

clarity. SHGC of the H₂O Nanofluid and Al₂O₃ Nanofluid performed equally less than baseline, but during trail experiments it appeared that sensible heat gains in the meter chamber was absorbed by the Nanowindow when couple with a larger heat exchanger. This resulted in a cooling effect previously not observed.

The Nanowindow was scaled to have meaningful impact as a renewable technology. Applying Ohm's Law derived that 1.3 million sqft of Nanowindows coupled with 33,800sqft of thermoelectric generators results in 18,100 W (18 kW)⁶ of electricity, service 14 homes, take 2.4 cars off the street, and eliminates 13 tons of CO₂. While the impact may not be as significant as photovoltaics it illustrates that Nanowindow possess the potential to be considered as a renewable technology alternative with viable beginnings no different than the first silicon cells of Bell Labs. The potential for window gap technology to shift from resisting energy to harnessing solar energy presented a unique opportunity to turn windows into energy brokers, and advance zero net energy goals. Glass skyscrapers may have one more renewable option to turn vertical real estate into energy generators without degrading visible transmittance and offering multiple energy offsets for heating, cooling, and energy generation. The emerging technology established a durable foundation to continue evaluating optical clarity and high-performance characteristics of nanofluids.

FUTURE WORK

It was observed that circulating nanofluids reduced transmitted irradiance levels compared to nanofluids fluids at rest. The absorption of water was a fundamental property that influenced the passage of light through the water column (Pegau & Zaneveld, 1993, p. 188), and that the absorption spectrum of the water column in the Nanowindows changes with an increase in temperature (Collins, 1925, p. 772). The cause of this resided within the microscopic changes in water structure that occurred as the temperature increased (Langford, McKinley, & Quickenden, 2001, p. 8921) causing covalent bonds of the water molecule to produce vibrations that absorbed spectral radiation at varying wavelengths. While this was not the focus of the research, it offered unique advantages that a nanofluid column may have on limiting various portions of the solar spectrum to protect indoor occupants from harmful wavelengths. Future experiments may explore the ultra violet protection offered by nanofluids.

Larger heat exchangers coupled with Nanowindows illustrated an unforeseen benefit that offered cooling potential. It was noted that the climate chamber's ambient temperature dropped as a function of the increased size of the heat exchanger. It is assumed that the Nanowindow can reduce the amount of incoming solar thermal energy entering the adjacent space, and absorb sensible heat in that space as a ratio of heat exchanger-to-Nanowindow size.

ACKNOWLEDGMENTS

Sincere gratitude goes out to G.Z. Brown, Funding Director of the Energy Studies in Buildings Laboratory at the University of Oregon; Dr. Ihab Elzeyadi; Dr. Pablo La Roche; and Dr. Kelly Sutherland for their support in the preparation of this manuscript. Special thanks to Frank Smith with the Lighting Lab at California State University, Pomona, Rich Wipfler at Eastman Chemical Company, Leif Ortegren at Pilkington BPNA, Nicholas Peak at Viracon, Walt Lutzke at Tubelite, Howard Eckstein at MCD Electronics Inc, David Conroy at NASA Jet Propulsion Laboratory, and Dr. Jason Rama at Meliorum Technologies, Inc.

⁶ Based on PVWatts the tilt angle was adjusted to 90-degrees to simulate a vertical solar panel. It was determining that there is a 40% degradation in energy production compared to 34-degrees. 18 kW takes into consideration 90-degree tilt.

EQUATIONS

$$1 \quad U = \frac{Q}{(T_{MC} - T_{CC})}$$

Where:

U = thermal transmittance (W/m²K)

Q = heat flow through the specimen (W/m²)

T_{MC} = Meter chamber ambient temperature (C°)

T_{CC} = Climate chamber ambient temperature (C°)

$$2 \quad VT = \frac{(\sum ti_{eog} + \sum ti_{cog}) \times 0.5}{\sum ii_{ss}}$$

Where:

$\sum ti_{eog}$ = sum of transmitted illuminance between 400nm - 750nm at the edge-of-glass

$\sum ti_{cog}$ = sum of transmitted illuminance between 400nm - 750nm at the center-of-glass

$\sum ii_{ss}$ = sum of incident illuminance between 400nm - 750nm as tested in Part 2

$$3 \quad SHGC = \frac{Q_{hf} - Q_{U-factor}}{A_{specimen} ii}$$

$SHGC$ = Solar Heat Gain Coefficient

Q_{hf} = Heat Flux (W/m²) as defined in Chapter IV

$Q_{U-factor}$ = Specimen U-factor as defined in Chapter II

ii = incident illuminance (W/m²) as defined in Chapter II

$$4 \quad \frac{Vd}{Va} = Nano_{Assembly}$$

Where :

$Vd_{(dc)}$ = Voltage Desired (vdc)

$Va_{(dc)}$ = Voltage Actual (vdc/sqft)

$Nano_{Assembly}$ = Nanowindow Assembly Size (sqft)

REFERENCES

- Aasteh, D., & Selkowitz, J. (1989). The Design and Testing of a Highly Insulating Glazing System for use with Conventional Window System. *ASME, Journal of Solar Engineering, III*.
- Burch, D. M., Licitra, B. A., & Zarr, R. R. (1990). A COMPARISON OF 2 TEST METHODS FOR DETERMINING TRANSFER-FUNCTION COEFFICIENTS FOR A WALL USING A CALIBRATED HOT BOX. *Journal of Heat Transfer, 112*(1), 35–42.
- Choi, S. U. S. (1998). *Nanofluid Technology: Current Status and Future Research*.
- Choi, S. U. S., Zhang, Z. G., Yu, W., Lockwood, F. E., & Grulke, E. A. (2001). Anomalous thermal conductivity enhancement in nanotube suspensions. *Applied Physics Letters, 79*(14), 2252. <https://doi.org/10.1063/1.1408272>
- Collins, J. R. (1925). Change in the infra-red absorption spectrum of water with temperature. *Physical Review, 26*(6), 771.
- Finlayson, E. U., Arasteh, D. K., Huizenga, C., Rubin, M. D., & Reilly, M. S. (1993, July). WINDOW 4.0: Documentation of Calculation Procedures. LBNL Energy and Environment Division.
- ISO 12567-1. (2010). Thermal performance of windows and doors -- Determination of thermal transmittance by the hot-box method -- Part 1: Complete windows and doors. ISO.
- Johnson, T. E. (1991). *Low-E glazing design guide*. Boston: Butterworth Architecture.
- Langford, V. S., McKinley, A. J., & Quickenden, T. I. (2001). Temperature Dependence of the Visible-Near-Infrared Absorption Spectrum of Liquid Water. *The Journal of Physical Chemistry A, 105*(39), 8916–8921. <https://doi.org/10.1021/jp010093m>
- Murshed, S. M. S. (2005). Enhanced thermal conductivity of TiO₂ - water based nanofluids. *International Journal of Thermal Sciences, 44*(4).
- Pegau, W. S., & Zaneveld, J. R. (1993). Temperature-dependent absorption of water in the red and near-infrared portions of the spectrum. Retrieved from <http://ir.library.oregonstate.edu/xmlui/handle/1957/17038>
- Shin, D., & Banerjee, D. (2011). Enhanced Specific Heat of Silica Nanofluid. *Journal of Heat Transfer, 133*(2), 024501. <https://doi.org/10.1115/1.4002600>

- Shin, D., & Banerjee, D. (2015). Enhanced thermal properties of SiO₂ nanocomposite for solar thermal energy storage applications. *International Journal of Heat and Mass Transfer*, 84, 898–902. <https://doi.org/10.1016/j.ijheatmasstransfer.2015.01.100>
- Zhou, S.-Q., & Ni, R. (2008). Measurement of the specific heat capacity of water-based Al₂O₃ nanofluid. *Applied Physics Letters*, 92(9), 093123. <https://doi.org/10.1063/1.2890431>